PNAS RESEARCH ARTICLE | CELL BIOLOGY

Orchestrated translation specializes dinoflagellate metabolism three times per day

Carl Bowazolo[a], Bo Song[b], Sonia Dorion[a], Mathieu Beauchemin[a,1], Samuel Chevrier[a], Jean Rivoal[a], and David Morse[a,2]

Edited by Ueli Schibler, University of Geneva, Sciences III, Geneva 4, Switzerland; received December 10, 2021; accepted June 10, 2022 by Editorial Board member Jeannie T. Lee

Many cells specialize for different metabolic tasks at different times over their normal ZT cycle by changes in gene expression. However, in most cases, circadian gene expression has been assessed at the mRNA accumulation level, which may not faithfully reflect protein synthesis rates. Here, we use ribosome profiling in the dinoflagellate *Lingulodinium polyedra* to identify thousands of transcripts showing coordinated translation. All of the components in carbon fixation are concurrently regulated at ZT0, predicting the known rhythm of carbon fixation, and many enzymes involved in DNA replication are concurrently regulated at ZT12, also predicting the known rhythm in this process. Most of the enzymes in glycolysis and the TCA cycle are also regulated together, suggesting rhythms in these processes as well. Surprisingly, a third cluster of transcripts show peak translation at approximately ZT16, and these transcripts encode enzymes involved in transcription, translation, and amino acid biosynthesis. The latter has physiological consequences, as measured free amino acid levels increase at night and thus represent a previously undocumented rhythm in this model. Our results suggest that ribosome profiling may be a more accurate predictor of changed metabolic state than transcriptomics.

daily rhythms | dinoflagellate | carbon fixation | bioluminescence | DNA synthesis

Significance

This manuscript shows that translational control of gene expression in the dinoflagellate *Lingulodinium* over the course of a daily light-dark cycle is extensive and sophisticated. The components of entire metabolic pathways can be regulated concurrently, and overall, protein synthesis occurs primarily at one of three different times of the day.

Many cells show changes in gene expression over a diel or circadian cycle (1, 2), suggesting that this allows them to specialize for different metabolic tasks at different times of the day. In several systems this has been shown to confer a selective advantage (3–5). The dinoflagellate *Lingulodinium* (formerly *Gonyaulax*) *polyedra* is a useful model system in which to address temporal metabolism and physiology as there are known daily rhythms in carbon fixation and bioluminescence that have been previously correlated with changes in translation of only a few key proteins (6–8). Furthermore, for other rhythms such as the nightly DNA replication, although no regulatory mechanism has yet been uncovered, the basic biochemistry of the process itself is known.

Examination of the biochemical bases for rhythms in the dinoflagellate *Lingulodinium* has shown that two distinctly different strategies are used. In one, increased protein synthesis rates result in increasing protein levels that correlate with onset of the rhythm. This is seen in the nightly bioluminescence rhythm, in which translation of two essential bioluminescence proteins, luciferase and luciferin-binding protein (LBP) (7, 9), at the beginning of the night increases both the amounts of the two proteins and the level of light emission. Levels of the two proteins vary in phase with the nightly light production because both proteins are specifically degraded at the end of the night phase as light emission decreases (6, 7). In a second scenario, increased protein synthesis rates are again observed at the onset of changes in physiological rhythms, but no changes in protein levels are observed. This observation has also been made in cyanobacteria, in which there are highly correlated changes in transcription and translation rates but no major changes in protein levels (10). These dampened changes in protein abundance have been proposed to result from slow protein turnover rates. In *Lingulodinium*, this is seen in the daily CO_2 fixation rhythm, in which increased synthesis of ribulose bisphosphate carboxylase/oxygenase (RuBisCO, catalyzing the rate-limiting step of carbon fixation) correlates with the increase in CO_2 fixation rate despite constant RuBisCO protein levels (8, 11, 12). RuBisCO appears to have a very low turnover rate (13), suggesting a possible mechanistic similarity to the low amplitude changes in cyanobacterial proteins over a diurnal cycle (10). These few specific examples show that changing translation rates of specific proteins is a useful marker for changes in dinoflagellate metabolism independent of changes in protein levels. However, they do not address the extent to which changes in gene expression occur, what aspects of cell metabolism may be subject to translation control, and how many times over the diel cycle that the cells are able to control the synthesis of specific proteins.

Author affiliations: [a]Institut de Recherche en Biologie Végétale, Département de Sciences Biologiques, Université de Montréal, Montréal, QC H1X 2B2, Canada; and [b]Shenzhen Branch, Guangdong Laboratory of Lingnan Modern Agriculture, Genome Analysis Laboratory of the Ministry of Agriculture and Rural Affairs, Agricultural Genomics Institute at Shenzhen, Chinese Academy of Agricultural Sciences, Shenzhen, China

Author contributions: C.B., M.B., and D.M. designed research; C.B., S.D., M.B., and S.C. performed research and experiments; C.B., B.S., S.D., S.C., J.R., and D.M. analyzed data; C.B., B.S., J.R., and D.M. wrote the paper; and J.R. and D.M. obtained funding.

The authors declare no competing interest.

This article is a PNAS Direct Submission. U.S. is a guest editor invited by the Editorial Board.

[1]Present address: Lallemand, Montréal, QC H4P 2R2, Canada.

[2]To whom correspondence may be addressed. Email: david.morse@umontreal.ca.

This article contains supporting information online at http://www.pnas.org/lookup/suppl/doi:10.1073/pnas.2122335119/-/DCSupplemental.

Published July 18, 2022.

Lingulodinium has a circadian clock that is physiologically similar to other organisms, but for which the mechanism is completely unknown. Thus, instead of trying to understand this distal control over the daily behavior of the cells, our focus has been to understand the proximal causes of the daily rhythms observed. *Lingulodinium* and other dinoflagellates show remarkably few differences in transcript abundance over a diel period (14, 15), so to date, transcriptomics has not yet provided any clues as to the metabolic capacity of cells at different times of the day. In addition, attempts to uncover global changes in protein levels by liquid chromatography-tandem mass spectrometry (LC-MS/MS) have also found few differences (12). Here, we have used ribosome profiling to gauge genome-wide changes in RNA translation rates. This technique counts the number of ribosome-protected fragments (RPFs) after nuclease digestion as a surrogate for genome-wide protein synthesis rate measurements (16, 17), and has been successfully used to assess daily rhythms in translation in several model systems (18–20). Since RNA translation rates are a common denominator in the two known strategies generating *Lingulodinium* rhythms, we hypothesized that ribosome profiling may provide a comprehensive picture as to the number, timing, and type of genes whose expression varies over the diel period in dinoflagellates. In this study, we identify thousands of regulated transcripts, with coordinated translation of almost all of the enzymes involved in carbon fixation, bioluminescence, glycolysis, and tricarboxylic acid TCA cycle pathways, as well as many of the components involved in DNA replication and gene expression. Unlike other systems in which changes in gene expression often occur principally at two different times (19, 20), we see peaks in the number of proteins synthesized around dawn (ZT0), around dusk (ZT12), and around ZT16. This latter unexpected cluster includes proteins involved in amino acid biosynthesis and appears to have physiological consequences, as measured free amino acid levels were found to increase at night. These findings clearly show an implication of translational control in known rhythms and allow the inference that many other biochemical processes may also vary over the daily cycle.

Results

Many Transcripts Are Differentially Translated over the Daily Cycle. To assess the ability of ribosome profiling to provide reliable information on changes in gene expression occurring at a translational level, we examined three times (Fig. 1*A*) where previous work using a different strain of the same species had identified high synthesis rates for four proteins (peridinin-chlorophyll a-protein [PCP] at ZT6, LBP at ZT14, and RuBisCO and glyceraldehyde-3-phosphate dehydrogenase [GAPDH] at ZT20) using in vivo [^{35}S]methionine labeling (21). We chose a light-dark cycle (ZT, where ZT0 is lights-on and ZT12 is lights-off) to identify all of the changes that may occur, so changes in synthesis rates will include both circadian and direct responses to changes in light intensity.

All of the samples contained the expected ∼30 base RPFs as determined by gel electrophoresis (*SI Appendix*, Fig. S1). Sequence analysis revealed the presence of two size classes of *Lingulodinium* RPF (*SI Appendix*, Fig. S2), and thus differs from the many examples in which only a single peak of RPF fragment sizes is observed (18, 19, 22). Two size classes of RPFs have been seen in yeast (23), but in yeast the second size class is smaller than 30 nt, unlike the slightly larger size seen with *Lingulodinium*. However, in both *Lingulodinium* and yeast, both size classes have similar read counts per transcript and both contain nuclear and organellar sequences (*SI Appendix*, Fig. S3). We do not find any significant difference in GC content between the small and large *Lingulodinium* RPF. However, we note that the average minimum free energy (24) of large RPFs (−5.02) is significantly smaller than that of the smaller RPFs (−1.62) ($P < 2.2\ e^{-16}$), suggesting that large RPFs may be a consequence of folded hairpins on mRNA.

Triplicate samples from any one time are well correlated and differ from samples taken from a different time (*SI Appendix*, Fig. S4 and Fig. 1*B*), and RPFs were distributed along the length of the LBP transcript at its peak synthesis time (ZT14), as expected (*SI Appendix*, Fig. S5). Furthermore, RPF counts at the three times agreed with what was expected for the four control proteins (*SI Appendix*, Table S4 and Fig. S6). Significant differences in RPFs were calculated for all pairwise comparisons of two times, then combined to yield a total of 3,324 transcripts, with significant differences in RPFs at one of the three sampling times. Roughly half of the transcripts with high RPFs at either ZT6 and ZT14 had high RPFs at two of the three times (Fig. 1*B*), while the majority of transcripts with high RPF at ZT20 had high RPF at two of the three times.

Since the overall correlation between triplicate samples was generally good (*SI Appendix*, Fig. S4), in a second experiment, a single sample was taken every 2 h (Fig. 1*A*) to assess the daily protein synthesis landscape at higher temporal resolution. Here, 3,326 transcripts were found to have significant differences in RPF levels with a 24-h periodicity using JTK_Cycle (*SI Appendix*, Table S5) (25). Of these, 1,020 transcripts were also present in the 3 times dataset; differences between the 2 experiments are likely due to the greater statistical power of triplicate samples in the first experiment, and to the imposition of a 24-h periodicity criterion in the second experiment. Interestingly, peak RPF levels for the different transcripts are not evenly distributed across the diel cycle, but are instead concentrated around three time windows: (1) a transition from dark to light (ZT0), (2) a transition from light to dark (ZT12), and (3) a time (ZT16) close to the middle of the night phase (Fig. 1*C*). These patterns are readily observed on a heat map after clustering (Fig. 1*D*).

To test the possibility that differences in RPF levels were related to RNA levels themselves, we compared RPF levels with previous measurements of RNA levels over the daily cycle by RNA sequencing (RNA-seq) (14), which had not shown any significant changes in RNA levels over four different times. When data from the previously measured RNA levels were compared directly to RPF levels, the timing and the magnitude of changes are clearly different (*SI Appendix*, Fig. S7). To further support a lack of change in RNA levels, two representative transcripts showing robust changes in RPF levels at ZT0, ZT12, and ZT16 were assayed by qRT-PCR and found not to vary (*SI Appendix*, Fig. S8). We conclude that changes in RPF levels reflect changes in the translation of the different transcripts.

Although the higher temporal resolution experiment finds three times in which large numbers of transcripts are translated, these times do not directly correspond to the times selected for the first experiment, so this may also contribute to differences in the sequences identified by the two experiments. However, changes in RPF values again compare favorably to in vivo [^{35}S]methionine incorporation for the four previously characterized proteins (21) (*SI Appendix*, Fig. S6), as well as to the time of increasing protein levels for 13 proteins recently identified by LC-MS/MS to vary in amount over the ZT cycle (*SI Appendix*, Fig. S9) (12). We conclude that RPF data are a good surrogate for changing protein synthesis rates. Interestingly, a test for enrichment of potential regulatory sequences in

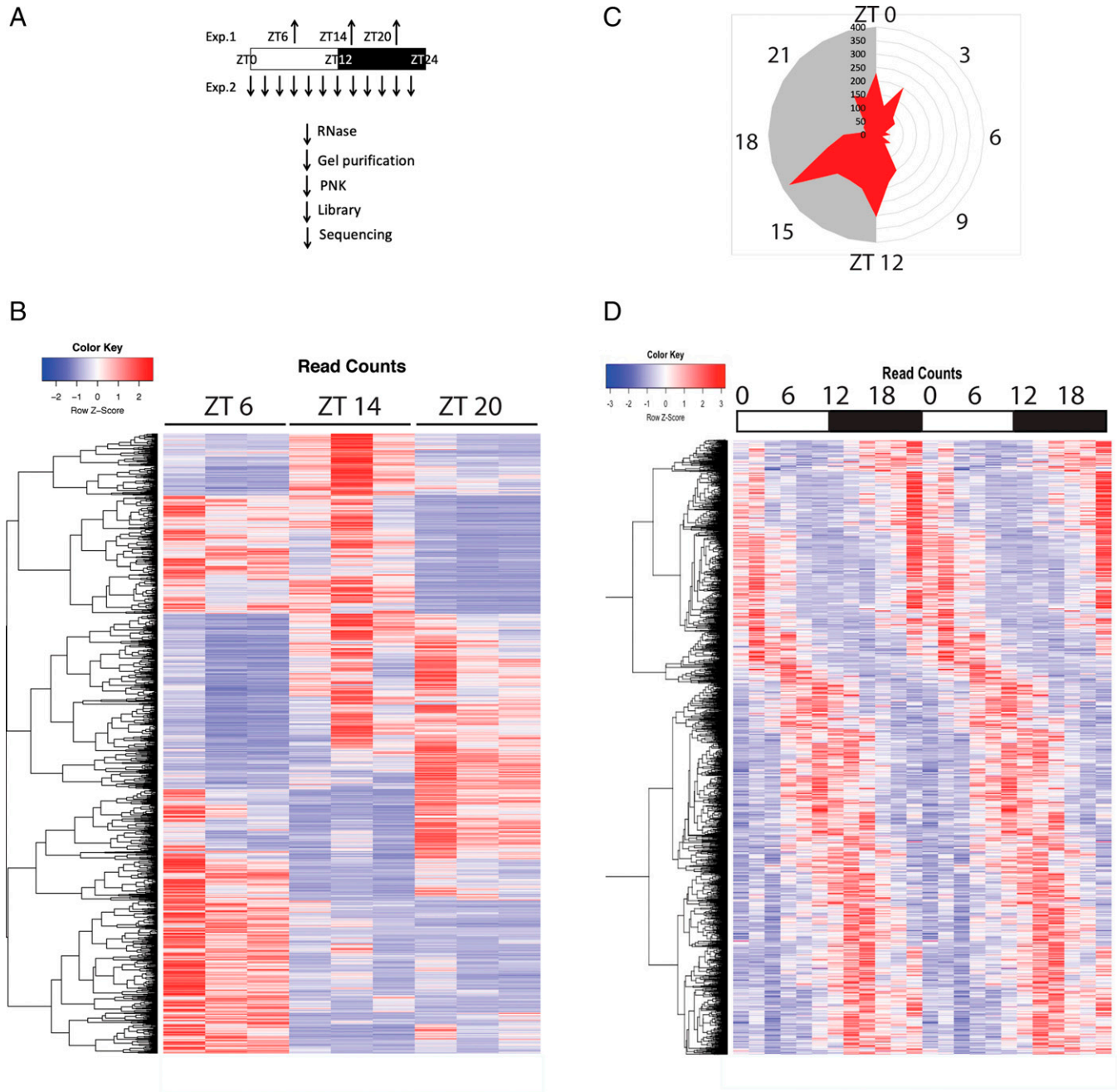

Fig. 1. A complex temporal landscape of protein synthesis rates with three peak times. Two experiments with different temporal resolutions were tested, one at roughly 8-h intervals (Exp. 1) and the other at 2-h intervals (Exp. 2). ZT0 corresponds to dawn (*A*). A total of 3,324 significant ($p_{adj} < 0.05$) differences (as determined by pairwise comparisons of time points using DESeq2) between triplicate samples at the three times are shown as a clustered heatmap, with transcriptome entries represented by horizontal lines and RPF read counts on a color scale (*B*). For the 2-h time-resolution experiment, the number of significant transcripts (Benjamini-Hochberg $q < 0.05$; amplitude change >2), with a 24-h rhythmic period peaking at each time (h, as determined by JTK cycle) is shown (*C*). Double-plotted read counts for 3,326 transcripts indicate three major phases of protein synthesis, two of which roughly coincide with transitions between light and dark (*D*).

transcripts with peak synthesis around lights-on revealed an enrichment of GC-rich motifs not observed in transcripts synthesized at other times (*SI Appendix*, Table S6), suggesting the possibility of common regulatory mechanisms for at least some groups of transcripts.

Many Transcripts Translated Near Dawn Precede the Known Day Phase Photosynthesis Rhythm. During the light period, cells have specialized for photosynthesis, and we hypothesized that proteins involved in this process may be among those whose peak synthesis occurred at approximately ZT0. Indeed, photosynthesis, carbon fixation, and the pentose phosphate shunt are among the principal Gene Ontology (GO) categories significantly enriched at ZT6 in the 3 times experiment (*SI Appendix*, Fig. S10). In the GO category for photosynthetic light reactions, including photosystem proteins, light-harvesting proteins, and ferredoxin, all of the proteins with significant differences show their peak synthesis rates beginning just before lights-on and continuing through the day phase (*SI Appendix*, Fig. S11). The peak time for synthesis of all 13 enzymes involved in carbon fixation (Fig. 2*A*) is more circumscribed than is observed for the photosynthesis proteins, with a more

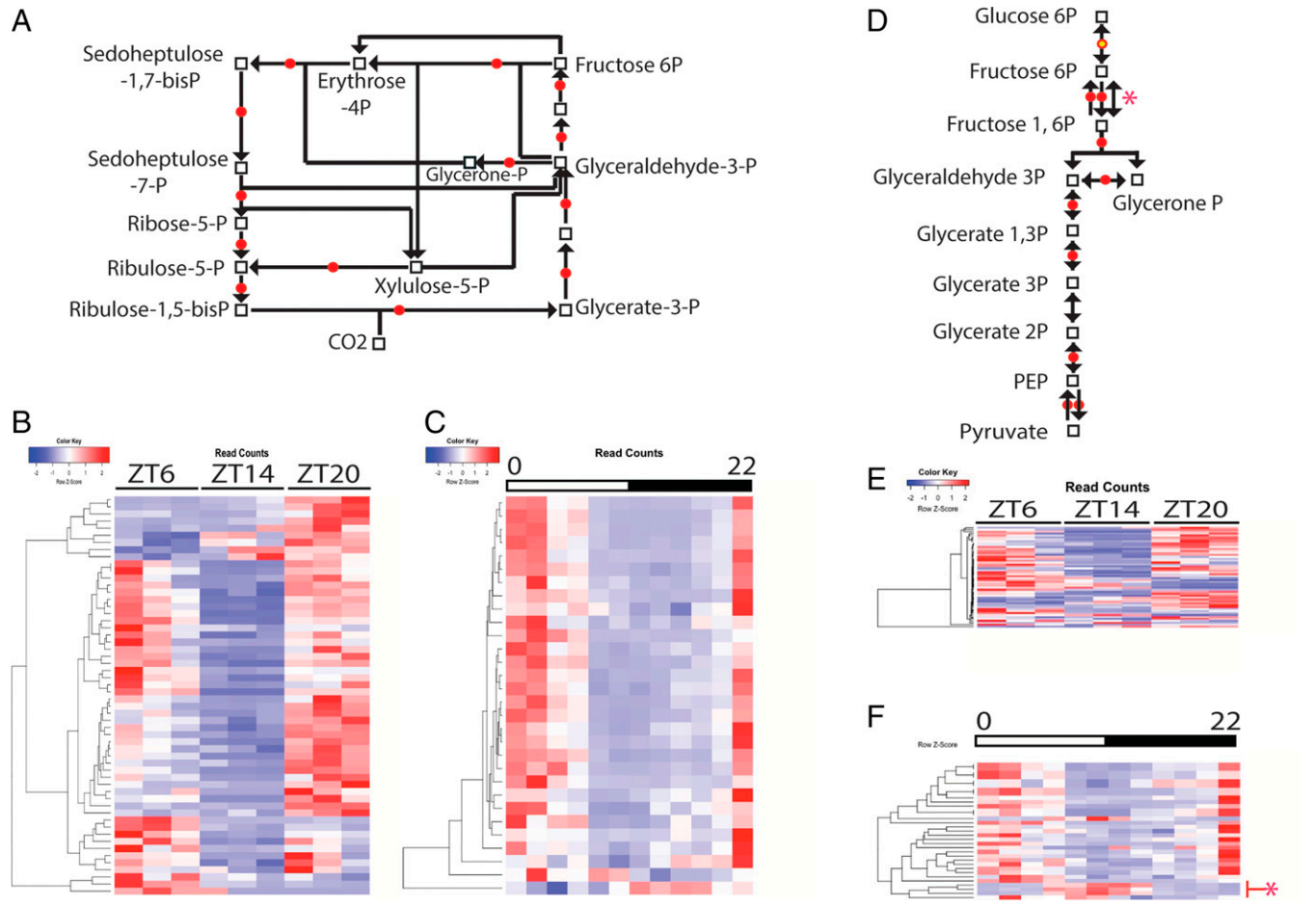

Fig. 2. Enzymes involved in carbon metabolism are regulated around ZT0. A schematic view of carbon fixation (from Kyoto Encyclopedia of Genes and Genomes [KEGG] map 00710) showing enzymes whose translation is regulated as red circles, and metabolites as gray squares (*A*). Heatmaps show that all enzymes are concurrently regulated in the 3-times (*B*) and in the 12-times experiments (*C*) and that increased synthesis precedes lights-on. A schematic view of glycolysis/gluconeogenesis (from KEGG map 00010) shows enzymes whose translation is regulated as red circles and enzymes found in the transcriptome but whose synthesis is unregulated as yellow circles (*D*). A reversible reaction catalyzed by a PFP is marked by a red asterisk in both the schema and the heatmap at *Bottom*. The heat maps for the 3-times (*E*) and 12-times (*F*) experiments show the same timing patterns as for carbon fixation.

sharply defined peak of translation centered around ZT0. Note that sequences whose synthesis rate peaks occur at ZT22, ZT0, and ZT2 are observed in the heat maps for both carbon fixation and glycolysis (Fig. 2*C* and *F*), indicating that this group should be considered as a single cluster. The increased translation occurring just before lights-on suggests a potential for circadian control over this process, and while not pursued here, circadian control has been documented for one of these enzymes, ribulose bisphosphate carboxylase/oxygenase (*SI Appendix*, Fig. S6) (21). A similar pattern of synthesis rate changes was seen for 9 of 12 enzymes in the glycolysis/gluconeogenesis pathway (compare Fig. 2*B* and *E*, *C* and *F*). Of the three other enzymes in the glycolytic pathway, one was not in the transcriptome, one was not regulated, and the last, a pyrophosphate fructose-6-phosphate phosphotransferase (PFP; Fig. 2, red asterisks), was regulated but with peak synthesis times around the onset of darkness. Interestingly, PFP uses pyrophosphate instead of adenosine triphosphate (ATP) as a substrate, so the PFP-catalyzed reaction may support metabolic flux through glycolysis at night due to pyrophosphate production by the nightly DNA synthesis (see below). PFP is also used in the pentose phosphate pathway, which generates NADPH in a parallel pathway to glycolysis, although all of the other regulated enzymes in this pathway show peak synthesis around ZT0, similar to carbon fixation (*SI Appendix*, Fig. S12). Overall, the degree to which coordinated translation of enzymes in these common metabolic pathways occurs is striking when compared with a ribosomal profiling experiment in *Arabidopsis* (20), where only three glycolytic enzymes and one Calvin cycle enzyme were found to be regulated.

Increased glycolytic flux during the day would be expected to produce both reducing power and pyruvate, which can fuel fatty acid synthesis, the latter by conversion to acetyl-coenzyme A (CoA). In agreement with this, fatty acid biosynthetic enzymes also show peaks in translation around ZT0 (*SI Appendix*, Fig. S13), suggesting that accumulation of fatty acids during the day may store energy produced by photosynthesis. This suggestion is supported by the increased translation of two enzymes involved in fatty acid degradation around ZT12 (*SI Appendix*, Fig. S13). While daily rhythms in fatty acid levels have not been reported, extensive sequestration of fixed carbon in triglycerides has been observed after nitrate deprivation, indicating that cells can store photosynthetically fixed carbon in this form (26). Starch, another potential reserve of fixed carbon, has been observed to accumulate during the day and to disappear during the night (26). There are few regulated enzymes in the starch metabolic pathway, but two enzymes for starch production (starch synthase and starch branching enzyme) are synthesized at dawn, while starch phosphorylase, catalyzing starch degradation, is synthesized at dusk (*SI Appendix*, Fig. S14). Enzymes involved in the biosynthesis of cellulose are also rhythmically translated, but this storage form of fixed carbon is unlikely to act as an energy reserve, as translation of biosynthetic enzymes is restricted to ZT22 (*SI Appendix*, Fig. S15).

It seems more likely that cellulose biosynthesis will be used to form new cellulosic thecal plates (27) that surround the cell and must be created for cytokinesis at ZT1. In addition to glucose, several enzymes involved in fructose and mannose production appear regulated, with all enzymes (except for PFP, as noted above) preferentially translated around ZT0 (*SI Appendix*, Fig. S16). The protein synthesis patterns seen in Fig. 2 are also seen when only sequences common between the two experiments are used (*SI Appendix*, Fig. S17). Taken together, a specialization for photosynthesis and carbon metabolism during the day agrees well with increased translation around ZT0 of multiple enzymes in the relevant pathways.

Many Transcripts Translated at Dusk Precede Known Night Phase Rhythms. In contrast to day phase cells, night phase cells specialize for bioluminescence (7) and DNA replication (28). Bioluminescence peaks at midnight, and the only two known proteins involved (luciferase and LBP) are concurrently translated, with peak synthesis rates centered around ZT12 (Fig. 3*A* and *B* and *SI Appendix*, Fig. S9). DNA replication begins at midnight and is among the principal GO categories significantly enriched at ZT14 using Fisher's exact test in the three-times experiment (*SI Appendix*, Fig. S18). The peak translation time for the majority of regulated proteins involved in DNA replication and repair is around ZT12 in the 12-times experiment (Fig. 3*D* and *E*). Interestingly, the proteins involved include not only the DNA polymerase, primase, and the MCM proteins but also a dinoflagellate/viral nucleoprotein (29), a major basic nuclear protein that has replaced histones in compacting DNA, and is responsible for the unusual dinoflagellate chromatin structure (30). Translation rates of the DNA clamp protein, proliferating cell nuclear antigen (PCNA), are high at a

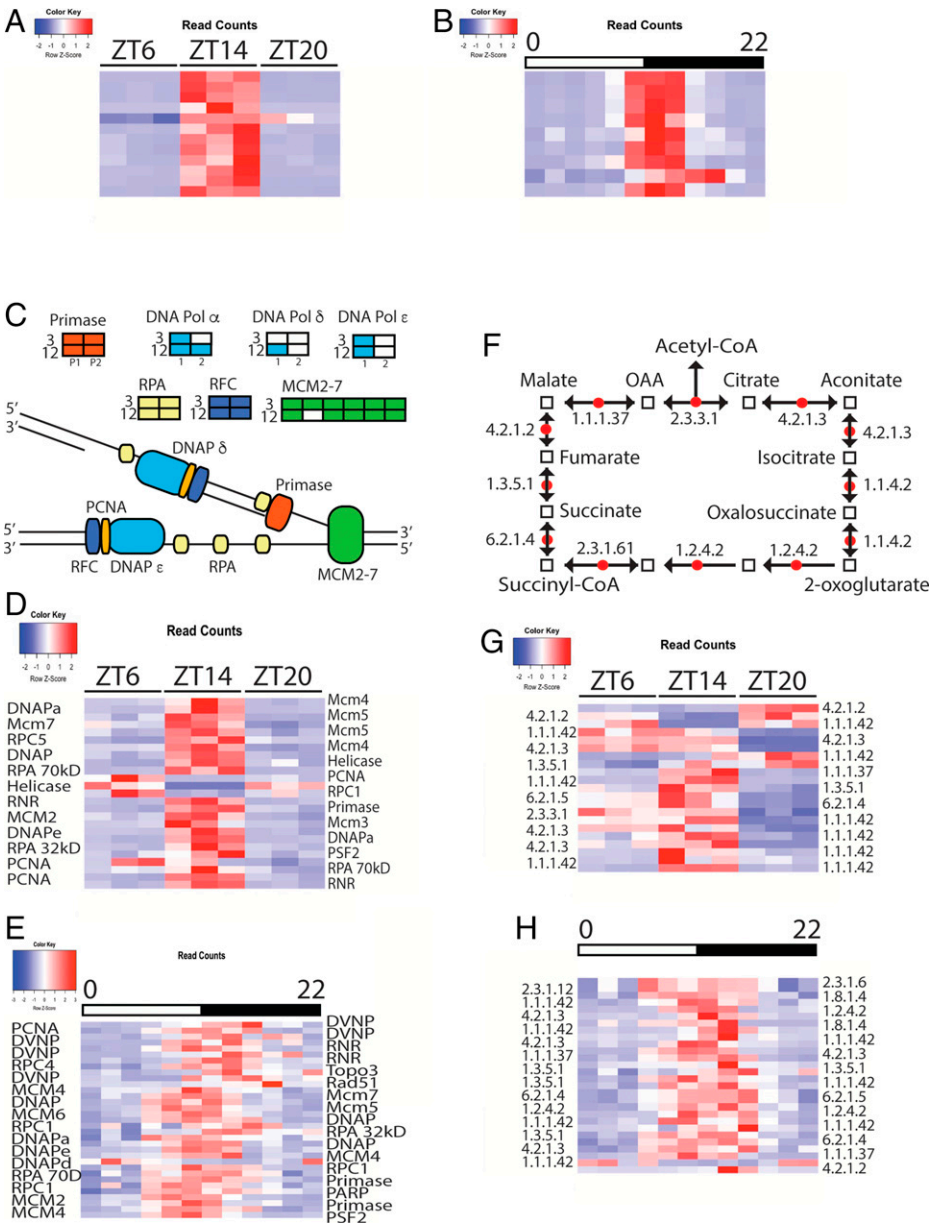

Fig. 3. Known night-phase rhythms are concurrently regulated around ZT12. Synthesis rates for all transcripts encoding the two bioluminescence proteins are maximal at the onset of the night phase (*A*, *B*). A schematic view of DNA replication shows enzymes found in the transcriptome as rectangles, with colored rectangles representing regulated sequences (*C*). The timing of translation for all sequences, with significant differences involved in replication and repair is similar in both the 3-times and 12-times experiments (*D*, *E*). A schematic view of the TCA cycle (from KEGG map 00020) shows metabolites as white squares and regulated enzymes as red circles (*F*). The timing of transcript translation for both experiments (*G*, *H*) is similar to DNA replication.

time when measured PCNA protein levels are increasing (12) (*SI Appendix*, Fig. S9). Curiously, few enzymes involved in purine and pyrimidine biosynthesis were found to be regulated (*SI Appendix*, Figs. S19 and S20), with most of the regulated enzymes in these pathways involved in interconverting the various phosphorylated forms of the different nucleotides. The TCA cycle also appears as a GO category enriched at ZT14 in the three-times experiment (*SI Appendix*, Fig. S18). All of the steps catalyzed by enzymes present in the transcriptome are regulated (Fig. 3*F*), and in both experiments (Fig. 3*G* and *H*), the pattern of protein synthesis rates is remarkably similar to what was observed for proteins involved in DNA replication. Nightly increases in the levels of two TCA cycle enzymes have been previously reported, with at least one regulated by the circadian clock at a translational level (31). It is thus possible that metabolic flux through the TCA cycle increases during the night phase, and may provide energy for DNA synthesis by aerobic metabolism. Starch-degrading enzymes show increased translation rates during late day/early night phase (*SI Appendix*, Fig. S14), suggesting that starch may be the carbon storage used to fuel aerobic metabolism. Pyruvate is the direct source of acetyl-CoA for the TCA cycle, and pyruvate production by glycolysis at night may be aided by PFP, a glycolytic enzyme using pyrophosphate as a phosphate donor (Fig. 2*F*). Examination of the pyruvate metabolic pathway indicated that enzymes playing a role only in pyruvate metabolism showed peak synthesis at ZT12, while enzymes also playing a role in other pathways had peak synthesis rates at ZT22 (*SI Appendix*, Fig. S21). The protein synthesis patterns seen for DNA synthesis and the TCA cycle in Fig. 3 are also seen when only sequences common between the two experiments are used (*SI Appendix*, Fig. S22). Thus, known day and night phase rhythms correspond to identified metabolic pathways whose members show increased protein synthesis rates at ZT0 and ZT12, respectively.

Some Transcripts Are Translated Preferentially after Dusk. The third identified peak in the number of regulated transcripts seen around ZT16 (Fig. 1*C*) was unexpected, as only two peaks of regulated transcripts were seen in *Arabidopsis* (20) and human cell cultures (19), and two major peaks were observed in murine liver (18) or kidney (32). To assess what metabolic processes may be specifically occurring at ZT16 in correlation with this peak, we examined the GO categories enriched at ZT20 (*SI Appendix*, Fig. S23). We eliminated categories such as sugar metabolism and photosynthesis, clearly associated with ZT0, reasoning that ZT20 (midway between ZT16 and ZT0) may contain categories from both ZT16 and ZT0. The remaining GO categories, potentially representing specific enrichment at ZT16, include the regulation of gene expression and biosynthetic/metabolic processes for 16 amino acids. We thus examined RPF values in the 12-times experiment for all of the sequences annotated as involved in transcription, translation, ribosome formation, aminoacyl-tRNA synthesis, and amino acid metabolism. The protein synthesis patterns for all of these categories were generally similar, with high translation rates between ZT14 and ZT16 (Fig. 4). This suggests that in addition to the previously characterized night phase rhythms, the cells may have a late night phase rhythm in gene expression.

Our current strain of *L. polyedra* does not take up radiolabeled amino acids from the external medium, precluding facile measurement of global protein synthesis rates, although a higher rate of global protein synthesis during the night has been reported for the species (33, 34). Instead, we measured levels of free amino acids to determine whether changing synthesis rates of enzymes involved in amino acid synthesis may affect cellular levels of these metabolites. Almost half (26 of 56) of the amino acid biosynthetic enzymes present in the transcriptome are regulated, as seen when individual sequences are superimposed on a schematic illustrating the various amino acid biosynthesis pathways (*SI Appendix*, Fig. S24). An attempt to identify enzymes that may catalyze rate-limiting steps is hampered by a lack of experimental evidence from dinoflagellates, although studies using higher plants suggest that some enzymes identified by regulated RPF may qualify. These include shikimate dehydrogenase (EC 1.1.1.25 (35)), indole-3-glycerol-phosphate synthase (EC 4.1.1.48 (36)), and serine hydroxymethyltransferase (EC 2.1.2.1 (37)) (*SI Appendix*, Fig. S25). Taken together, these results suggest that many amino acids would show increased levels during the night. To test this directly, the levels of 17 individual amino acids were measured at 4 times over the ZT cycle, and 15 of these were found to have their lowest values during mid- to late day (Fig. 5 and *SI Appendix*, Table S7). The increase in amino acid pool levels is mirrored by a general increase in RPF for amino acid biosynthetic enzymes (Fig. 5 and *SI Appendix*, Fig. S25). RPF measurements as a surrogate for mRNA translation rates have thus correctly predicted a physiological rhythm. Interestingly, preferential amino acid synthesis during the dark period would represent a previously unexpected aspect to N-metabolism. This process may be restricted to the late night phase to partition it temporally away from carbon metabolism during the light phase or to align amino acid production with increased protein synthesis. In any event, our data support the idea of a third metabolic specialization occurring the diel cycle, with increased levels of gene expression occurring between DNA synthesis and carbon metabolism.

Discussion

The data reported here show that large numbers of genes have increased translation rates at ZT0 (lights-on), ZT12 (lights-off) and ZT16, and this differs in several respects from other reports examining protein synthesis rates over the daily period. For example, both *Arabidopsis* (20) grown under ZT conditions and human U20S cell cultures synchronized with dexmethazone (19) show only two peaks in the number of translated genes, and these occur around midday and midnight. However, murine kidney (32) and liver (18) tissues showed two major peaks (ZT0 and ZT16) and one minor peak (ZT10) of translation. With the exception of the genes translated at ZT0 in the two mouse studies, peak translation times in other models appear less tied to light-dark transitions than in *Lingulodinium*.

The extent to which different pathways in *Lingulodinium* show coordinated translation of their different components is also striking, with entire pathways concurrently regulated in some cases (*SI Appendix*, Table S8). It is also of interest that these changes occur at a translational level (*SI Appendix*, Fig. S7), which may suggest an increased reliance in translational control on an organism with little variation in transcript levels over the daily cycle (14). Lastly, the finding that thousands of transcripts are regulated translationally while only 13 proteins were found to change in abundance (12) supports the contention that increased protein synthesis rates may not always increase protein levels. Studies with cyanobacteria that have documented a similar behavior (10) have led to the suggestion that allosteric regulatory mechanisms may be involved. However, further studies will be required to fully understand the link between protein synthesis and cell

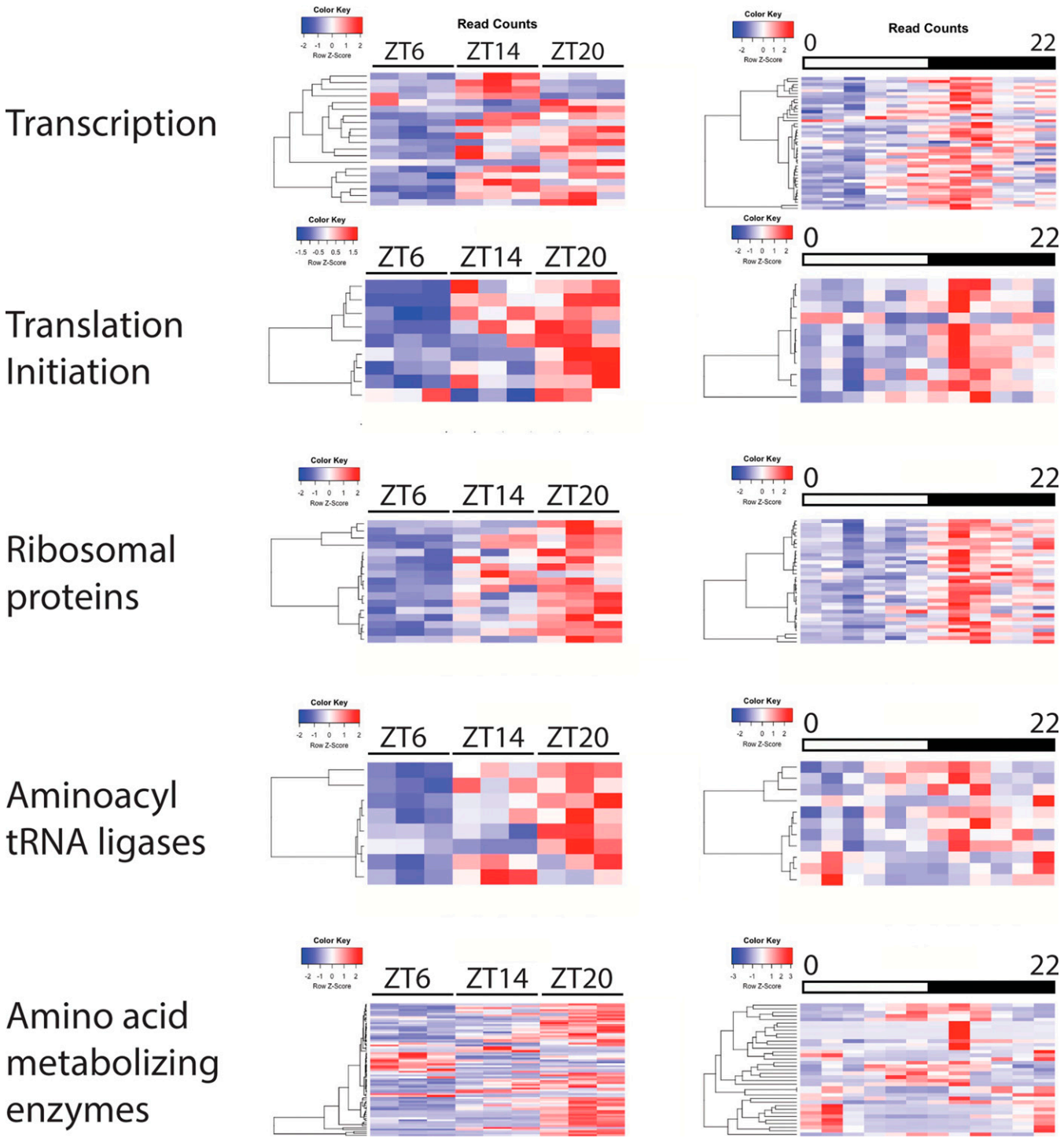

Fig. 4. Enzymes involved in the regulation of gene expression and amino acid biosynthesis are translated around ZT16. Enzymes involved in different aspects of gene expression were identified among regulated enzymes by GO annotations in both experiments. All appear regulated at a similar time close to the peak of proteins regulated at ZT16.

metabolism. In *Lingulodinium*, the relationship between high RuBisCO synthesis rates and high CO_2 fixation rates appears to involve a change in the distribution of RuBisCO within the chloroplasts themselves. High rates of CO_2 fixation occur when RuBisCO-enriched structures called pyrenoids form inside chloroplasts (8). Pyrenoids contain less of the major light-harvesting PCP, so carbon fixation efficiency is thought to increase because the oxygen-sensitive RuBisCO (38) becomes separated from the source of oxygen generation. New protein synthesis is important, as blocking protein transport to the plastid blocks both pyrenoid formation and the increase in CO_2 fixation (13).

Our results using RPF as a surrogate for protein synthesis rates in dinoflagellates indicate that this high-throughput method is likely to provide a more comprehensive picture of changes in metabolic activity than changes in transcript levels by RNA-seq. Ribosome profiling may be similarly important in other systems as a high-throughput method to identify potential metabolic changes. Importantly, our findings reveal that the metabolic specialization of dinoflagellates during a light-dark cycle is more sophisticated than a simple toggling between day and night phase states, an observation that should have important repercussions in the analysis of rhythmic phenomena in other systems.

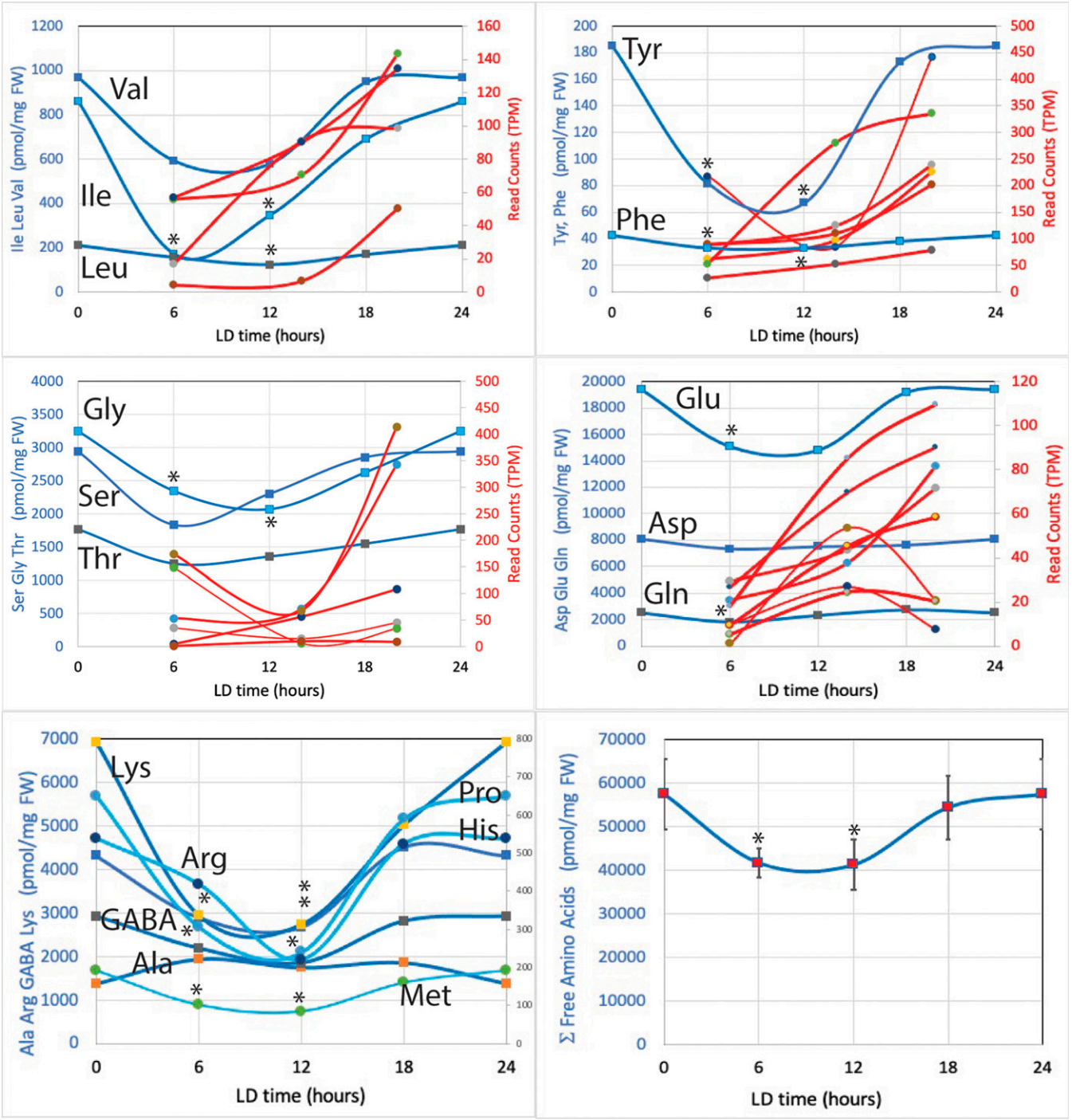

Fig. 5. Amino acid profiles over a daily cycle show increases during the dark phase. Average levels of amino acids (blue curves) were measured at four times over the daily cycle (n = 5, average error 15%), with ZT0 values duplicated at ZT24. Average read counts (transcripts per million [TPM], red curves) were determined from the 3-times experiments (n = 3, average error 20%) for KEGG pathway enzymes involved in the biosynthesis of the amino acids present in the transcriptome. Amino acid levels marked with an asterisk are significantly different from the levels at ZT0 ($P < 0.05$, Student's t test).

Materials and Methods

Cell Culture and Harvesting. *L. polyedra* (previously *Gonyaulax polyedra*) was obtained from the Provasoli-Guillard National Center for Marine Algae and Microbiota (East Boothbay, ME, USA) as culture CCMP1936. Cell cultures were grown in normal f/2 medium (39) prepared using Instant Ocean under a 12-h light (40 μmol photons m^{-2} s^{-1} cool white fluorescent light) and 12-h dark regime at a temperature of 18 °C ± 1 °C. This light-dark regime, called ZT, has ZT0 at lights-on and ZT12 at lights-off. After 2 min of pretreatment with cycloheximide (0.10 mM), 300 mL of cell suspension were harvested by filtration on Whatman 541 paper and scraped into 1.5-mL Eppendorf tubes containing 0.1 mm zirconium beads for cell disruption and immediately frozen in liquid nitrogen for storage at −80 °C until use.

Two experiments were performed. The first involved three time points in which samples were taken in triplicate. The three times were chosen because a previous study using *L. polyedra* strain 70 (CCMP1976), which readily took up radiolabeled amino acids from the culture medium, had identified three times with distinct patterns of protein synthesis rates. The PCP was synthesized at ZT6 (and not at ZT14 or ZT20), while LBP was synthesized at ZT14 (and not at ZT6 or ZT20), and RuBisCO and GAPDH were synthesized at ZT20 and not at ZT6 or ZT14. This experiment was designed to validate the procedure and to assess the fidelity between replicates. In the second experiment, 12 unique samples were

harvested every 2 h over the ZT cycle. This experiment was designed to assess the protein synthesis landscape at a higher temporal resolution.

Cell Lysis and Nuclease Digestion. The ribosome profiling procedure used was adapted from previously described protocols (40, 41) and involves ribonuclease digestion of RNA after cell lysis. RNA fragments protected from digestion by the presence of ribosomes (RPFs) are isolated and sequenced and the number of RPFs for each transcript is used as a surrogate for translational efficiency at the different times of the experiments. Briefly, Eppendorf tubes containing roughly 350,000 cells and beads were placed on ice and resuspended in 200 μL lysis buffer (1% Nonidet P-40, 200 mM K-acetate, 25 mM Hepes-KOH pH 7.2, 10 mM MgCl, 4 mM $CaCl_2$, and 3.5 μM cycloheximide) and lysed for 2 min in a bead beater (BioSpec Products). The supernatant, after 5 min centrifugation at 9,000 rpm (at 4 °C), was taken up in a new tube and K-acetate concentration adjusted to 100 mM by 1:1 dilution with water before the addition of 5 μL (250 U) RNase If (New England Biolabs). RNase If was chosen because a higher number of RPFs to transcripts known to be translated at ZT14 were produced compared to RNase T1 (*SI Appendix*, Table S1) from RNA isolated at ZT14. Tubes were incubated for 45 min at room temperature.

RNA Extraction. Tubes were put back on ice and then sequentially 1 mL TRIzol and 200 μL chloroform were added. After homogenization, the tubes were returned to room temperature for 2 to 3 min. They were then centrifuged for 15 min at 12,000 rpm (4 °C). The aqueous supernatant was recovered in a new tube and incubated with 500 μL isopropanol for 10 min at room temperature, then centrifuged for 10 min at 12,000 × *g* (4 °C). The RNA pellet was resuspended with 10 μL water for electrophoresis.

Gel Migration and RPF Excision on Gel. RNA loading buffer (5 μL 96% formamide, 2% 1 mg/mL bromophenol blue, and 2% 10 mM ethylenediaminetetraacetate [EDTA]) was added to the resuspended RNA pellet, incubated at 70 °C for 5 min, then loaded on a 10% acrylamide (29:1) 1× Tris-borate-EDTA (TBE) gel with 0.3 μg 10-bp ladder (Thermo Scientific). Samples were electrophoresed at 200 V for approximately 22 min, after which the gel was colored with ethidium bromide (0.5 μg/mL). In a key step for the procedure, bands at 30 nt visualized under UV light (*SI Appendix*, Fig. S1*A*) were excised with a clean razor blade and the piece of gel put in a 1.5-mL tube containing 400 μL 400 mM Na-acetate (pH 5.2). The tube was then frozen at −80 °C for 10 min.

RNA Extraction from Gels. The tube was thawed at 95 °C for 7 min and the piece of gel totally crushed with a sterile pipette tip. This was followed by 2 cycles of 7 min at 95 °C and a few moments of vortexing; then, the tube was centrifuged at maximum speed for 10 min. The supernatant was taken up in a tube containing 1 mL ethanol, incubated for 1 h at −20 °C, and centrifuged at 4 °C for 15 min at maximum speed. The pellet containing the RPFs was washed with 80% (vol/vol) ethanol and centrifuged again for 5 min. The supernatant was discarded and the pellet dried for the polynucleotide kinase (PNK) modification.

PNK Modification and Gel Migration. The pellet was resuspended in 144 μL water, 18 μL 10× PNK buffer (New England Biolabs; 700 mM Tris·HCl [pH 7], 100 mM $MgCl_2$, 50 mM dithiothreitol), 18 μL ATP (100 mM), and 2 μL PNK, and the tube incubated with shaking at 37 °C for 45 min. After the reaction, RNA was precipitated using ethanol as described (42). The RNA pellet was resuspended in 30 μL diethylpyrocarbonate water and the quantity determined using a NanoDrop spectrophotometer (MBI Lab equipment). A total of 20 μg were electrophoresed (*SI Appendix*, Fig. S1*B*) under the same conditions as the first gel, while the rest was stored at −80 °C. At this stage the sample was sent to Génome Québec Innovation Centre (Montréal, Canada) for library construction and sequencing (40). Sequencing was performed using an Illumina HiSeq deep sequencing protocol (43, 44). An average of 1.8 and 4 million RPF with hits to mRNA were recovered for samples in the first and the second experiment, respectively (*SI Appendix*, Tables S2 and S3).

Bioinformatics Analysis. The sequences in fastq format produced by the sequencing reaction were trimmed in Galaxy to remove the adapters using TrimGalore (*SI Appendix*, Fig. S2 and Tables S1–S3). The length of the sequences was determined in Geneious, and read distributions were made by mapping reads to selected reference sequences to verify the distribution. Read counts were determined using Salmon in Galaxy with a previously described Velvet assembly containing 74,655 sequences (45) and a Trinity assembly containing 114,492 sequences (46) (*SI Appendix*, Table S4). For the first experiment, using triplicate samples taken at each of three times (ZT 6, ZT14, and ZT 20), pairwise significant differences between all of the combinations of these three times were determined using DESeq running in R (*SI Appendix*, Fig. S3). All of the sequences with a $p_{adj} < 0.05$ were combined to form a single file containing 3,324 entries with at least 1 time showing a significant difference. In the second experiment, in which a single sample was taken every 2 h, data were tested for significant rhythmicity using JTK_cycle (25) running in R. All of the sequences with a 24-h period, an average read count greater than 1 per million, a Benjamini-Hochberg $q < 0.05$, and a fold change >2 were selected. A total of 3,326 sequences were identified, 1,034 of which were also found in the first experiment. Motif searching for 6 nucleotide sequences enriched in certain groups of transcripts against a background of 1,000 transcripts randomly sampled from the total set of transcripts was performed using DMINDA 2.0 (47).

Raw sequence data has been deposited in the Sequence Read Archive (SRA) under BioProject ID PRJNA69549.

Amino Acid Analysis. Cells were disrupted in 80% (vol/vol) ethanol using a bead beater followed by a 30-min extraction at 70 °C using a Büchi Rotavapor (26). The extract was brought to dryness and redissolved in 5 mL H_2O. This extract was then separated into neutral, cationic, and anionic fractions using tandem ion exchange chromatography as previously described (48). One-mL aliquots of the basic fractions were evaporated to dryness before resuspension in 100 μL 20% (vol/vol) acetonitrile in 20 mM HCl. A total of 20 μL of this solution was analyzed by high-performance liquid chromatography (HPLC) after derivatization with the AccQ reagent (Waters). The Waters HPLC system was controlled by the Empower Pro software and equipped with a 600 controller. Detection was done using the Waters 2996 Diode Array Detector. Amino acids were separated on a Waters AccQ●Tag Amino Acid Analysis column (3.9 × 150 mm) equipped with a Nova-Pak C18 precolumn cartridge (3.9 × 20 mm). Quantification was performed using calibration curves generated from commercial standards (Thermo Scientific and Sigma-Aldrich). Results were corrected for recovery using L-norvaline as an external standard.

qRT-PCR Analysis. qRT-PCR was performed by the Institut de Recherche en Immunologie et Cancerologie (Montréal), from cell extracts in TRIzol taken at 2-h intervals. Oligonucleotide primers were 5′-CGAGCCAACCATCAGGGATG-3′ and 5′-AAGGATGTGGCCTGTGGTG-3′ for phosphoglycerate kinase (GABP01040553), 5′-CCTCCTTCACCACGATCGTG-3′ and 5′-GAAAATCTCACGTTCGCGCC-3′ for triose phosphate isomerase (GABP01052300), 5′-GCTTGCGGATGACAAGTTCC-3′ and 5′-CGAACTTGCCCTTGATGCAG-3′ for PSF2 (GABP01020619), 5′-CCCGCAGCCTA CATCCATG-3′ and 5′-ATTTTGCAGTCGCTGGGAGG-3′ for fructose phosphotransferase (GABP01053021), 5′-GCTCGCTGACCCTCGTCT-3′ and 5′-GGCACCAGGAAGAG CGTG-3′ for the 60S L37 (GABP01034064), and 5′-AGGGAAAGTCAGGAGGG CT-3′ and 5′-TGGAGACGGAGGAGGAGAAG-3′ for IF1 (GABP01058717). Actin (GABP01016862) was used as a control with primers 5′-GCTTTTCCAGCCGAG TTTGG-3′ and 5′-GCGGATATCGACATCGCACT-3′.

Data and Materials Availability. Raw sequence data used for this study has been deposited in the National Center for Biotechnology Information (NCBI) SRA under BioProject ID PRJNA69549.

Sequence reads data have been deposited in NCBI (BioProject ID PRJNA69549).

ACKNOWLEDGMENTS. We thank Drs. B.F. Lang, R. Maranger, and D. Kierzkowski for their critical comments on the manuscript before submission and C. Veilleux-Trinh for help with sample collection. Portions of this paper were developed from the thesis of C.B. (Université de Montréal, Montréal, Canada). We thank the National Science and Engineering Research Council of Canada for financial support (Discovery Grants 227271, to J.R., and 171382, to D.M.) and the National Natural Science Foundation of China (grant no. 31601042, to B.S.).

1. S. L. Harmer *et al.*, Orchestrated transcription of key pathways in *Arabidopsis* by the circadian clock. *Science* **290**, 2110–2113 (2000).
2. R. Zhang, N. F. Lahens, H. I. Ballance, M. E. Hughes, J. B. Hogenesch, A circadian gene expression atlas in mammals: Implications for biology and medicine. *Proc. Natl. Acad. Sci. U.S.A.* **111**, 16219–16224 (2014).
3. Y. Ouyang, C. R. Andersson, T. Kondo, S. S. Golden, C. H. Johnson, Resonating circadian clocks enhance fitness in cyanobacteria. *Proc. Natl. Acad. Sci. U.S.A.* **95**, 8660–8664 (1998).
4. A. N. Dodd *et al.*, Plant circadian clocks increase photosynthesis, growth, survival, and competitive advantage. *Science* **309**, 630–633 (2005).

5. K. Spoelstra, M. Wikelski, S. Daan, A. S. Loudon, M. Hau, Natural selection against a circadian clock gene mutation in mice. *Proc. Natl. Acad. Sci. U.S.A.* **113**, 686–691 (2016).
6. C. H. Johnson, J. F. Roeber, J. W. Hastings, Circadian changes in enzyme concentration account for rhythm of enzyme activity in *gonyaulax*. *Science* **223**, 1428–1430 (1984).
7. D. Morse, P. M. Milos, E. Roux, J. W. Hastings, Circadian regulation of bioluminescence in *Gonyaulax* involves translational control. *Proc. Natl. Acad. Sci. U.S.A.* **86**, 172–176 (1989).
8. N. Nassoury, L. Fritz, D. Morse, Circadian changes in ribulose-1,5-bisphosphate carboxylase/oxygenase distribution inside individual chloroplasts can account for the rhythm in dinoflagellate carbon fixation. *Plant Cell* **13**, 923–934 (2001).
9. M. Mittag, L. Li, J. W. Hastings, The mRNA level of the circadian regulated *Gonyaulax* luciferase remains constant over the cycle. *Chronobiol. Int.* **15**, 93–98 (1998).
10. J. Karlsen, J. Asplund-Samuelsson, M. Jahn, D. Vitay, E. P. Hudson, Slow protein turnover explains limited protein-level response to diurnal transcriptional oscillations in cyanobacteria. *Front. Microbiol.* **12**, 657379 (2021).
11. H. C. Hollnagel, E. Pinto, D. Morse, P. Colepicolo, The oscillation of photosynthetic capacity in *Gonyaulax polyedra* is not related to differences in Rubisco, peridinin or chlorophyll *a* amounts. *Biol. Rhythm Res.* **33**, 443–458 (2002).
12. C. Bowazolo *et al.*, Label-free MS/MS analyses of the dinoflagellate *Lingulodinium* identifies rhythmic proteins facilitating adaptation to a diurnal LD cycle. *Sci. Total Environ.* **704**, 135430 (2020).
13. N. Nassoury, Y. Wang, D. Morse, Brefeldin a inhibits circadian remodeling of chloroplast structure in the dinoflagellate gonyaulax. *Traffic* **6**, 548–561 (2005).
14. S. Roy *et al.*, The *Lingulodinium* circadian system lacks rhythmic changes in transcript abundance. *BMC Biol.* **12**, 107 (2014).
15. B. Zaheri, S. Dagenais-Bellefeuille, B. Song, D. Morse, Assessing Transcriptional Responses to Light by the Dinoflagellate *Symbiodinium*. *Microorganisms* **7**, 261 (2019).
16. N. T. Ingolia, Genome-wide translational profiling by ribosome footprinting. *Methods Enzymol.* **470**, 119–142 (2010).
17. N. T. Ingolia, Ribosome footprint profiling of translation throughout the genome. *Cell* **165**, 22–33 (2016).
18. P. Janich, A. B. Arpat, V. Castelo-Szekely, M. Lopes, D. Gatfield, Ribosome profiling reveals the rhythmic liver translatome and circadian clock regulation by upstream open reading frames. *Genome Res.* **25**, 1848–1859 (2015).
19. C. Jang, N. F. Lahens, J. B. Hogenesch, A. Sehgal, Ribosome profiling reveals an important role for translational control in circadian gene expression. *Genome Res.* **25**, 1836–1847 (2015).
20. A. Missra *et al.*, The circadian clock modulates global daily cycles of mRNA ribosome loading. *Plant Cell* **27**, 2582–2599 (2015).
21. P. Markovic, T. Roenneberg, D. Morse, Phased protein synthesis at several circadian times does not change protein levels in *Gonyaulax*. *J. Biol. Rhythms* **11**, 57–67 (1996).
22. F. Atger *et al.*, Circadian and feeding rhythms differentially affect rhythmic mRNA transcription and translation in mouse liver. *Proc. Natl. Acad. Sci. U.S.A.* **112**, E6579–E6588 (2015).
23. L. F. Lareau, D. H. Hite, G. J. Hogan, P. O. Brown, Distinct stages of the translation elongation cycle revealed by sequencing ribosome-protected mRNA fragments. *eLife* **3**, e01257 (2014).
24. R. Lorenz *et al.*, ViennaRNA package 2.0. *Algorithms Mol. Biol.* **6**, 26 (2011).
25. M. E. Hughes, J. B. Hogenesch, K. Kornacker, JTK_CYCLE: An efficient nonparametric algorithm for detecting rhythmic components in genome-scale data sets. *J. Biol. Rhythms* **25**, 372–380 (2010).
26. S. Dagenais Bellefeuille, S. Dorion, J. Rivoal, D. Morse, The dinoflagellate *Lingulodinium polyedrum* responds to N depletion by a polarized deposition of starch and lipid bodies. *PLoS One* **9**, e111067 (2014).
27. W. S. Chan, A. C. M. Kwok, J. T. Y. Wong, Knockdown of dinoflagellate cellulose synthase *CesA1* resulted in malformed intracellular cellulosic thecal plates and severely impeded cyst-to-swarmer transition. *Front. Microbiol.* **10**, 546 (2019).
28. S. Dagenais-Bellefeuille, T. Bertomeu, D. Morse, S-phase and M-phase timing are under independent circadian control in the dinoflagellate *Lingulodinium*. *J. Biol. Rhythms* **23**, 400–408 (2008).
29. S. G. Gornik *et al.*, Loss of nucleosomal DNA condensation coincides with appearance of a novel nuclear protein in dinoflagellates. *Curr. Biol.* **22**, 2303–2312 (2012).
30. N. A. T. Irwin *et al.*, Viral proteins as a potential driver of histone depletion in dinoflagellates. *Nat. Commun.* **9**, 1535 (2018).
31. H. Akimoto, T. Kinumi, Y. Ohmiya, Circadian rhythm of a TCA cycle enzyme is apparently regulated at the translational level in the dinoflagellate *Lingulodinium polyedrum*. *J. Biol. Rhythms* **20**, 479–489 (2005).
32. V. Castelo-Szekely, A. B. Arpat, P. Janich, D. Gatfield, Translational contributions to tissue specificity in rhythmic and constitutive gene expression. *Genome Biol.* **18**, 116 (2017).
33. G. Cornelius, A. Schroeder-Lorenz, L. Rensing, Circadian-clock control of protein synthesis and degradation in *Gonyaulax polyedra*. *Planta* **166**, 365–370 (1985).
34. B. Donner, U. Helmboldt-Caesar, L. Rensing, Circadian rhythm of total protein synthesis in the cytoplasm and chloroplasts of *Gonyaulax polyedra*. *Chronobiol. Int.* **2**, 1–9 (1985).
35. L. Ding *et al.*, Functional analysis of the essential bifunctional tobacco enzyme 3-dehydroquinate dehydratase/shikimate dehydrogenase in transgenic tobacco plants. *J. Exp. Bot.* **58**, 2053–2067 (2007).
36. J. Ouyang, X. Shao, J. Li, Indole-3-glycerol phosphate, a branchpoint of indole-3-acetic acid biosynthesis from the tryptophan biosynthetic pathway in *Arabidopsis thaliana*. *Plant J.* **24**, 327–333 (2000).
37. P. Mishra *et al.*, Heterologous expression of serine hydroxymethyltransferase-3 from rice confers tolerance to salinity stress in *E. coli* and *Arabidopsis*. *Front. Plant Sci.* **10**, 217 (2019).
38. S. Whitney, T. Andrews, The CO_2/O_2 specificity of single-subunit ribulose-bisphosphate carboxylase from the dinoflagellate *Amphidinium carterae*. *Aust. J. Plant Physiol.* **25**, 131–138 (1998).
39. R. R. L. Guillard, M. D. Keller, "Culturing dinoflagellates" in *Dinoflagellates*, D. M. Spector, ed. (Academic Press, Orlando, FL, 1984), pp. 412–417.
40. D. W. Reid, S. Shenolikar, C. V. Nicchitta, Simple and inexpensive ribosome profiling analysis of mRNA translation. *Methods* **91**, 69–74 (2015).
41. N. T. Ingolia, G. A. Brar, S. Rouskin, A. M. McGeachy, J. S. Weissman, The ribosome profiling strategy for monitoring translation in vivo by deep sequencing of ribosome-protected mRNA fragments. *Nat. Protoc.* **7**, 1534–1550 (2012).
42. S. E. Walker, J. Lorsch, RNA purification–precipitation methods. *Methods Enzymol.* **530**, 337–343 (2013).
43. J. Podnar, H. Deiderick, G. Huerta, S. Hunicke-Smith, Next-generation sequencing RNA-seq library construction. *Curr. Protoc. Mol. Biol.* **106**, 4.21.1–4.21.19 (2014).
44. M. A. Quail *et al.*, A large genome center's improvements to the Illumina sequencing system. *Nat. Methods* **5**, 1005–1010 (2008).
45. M. Beauchemin *et al.*, Dinoflagellate tandem array gene transcripts are highly conserved and not polycistronic. *Proc. Natl. Acad. Sci. U.S.A.* **109**, 15793–15798 (2012).
46. S. Roy, L. Letourneau, D. Morse, Cold-induced cysts of the photosynthetic dinoflagellate *Lingulodinium polyedrum* have an arrested circadian bioluminescence rhythm and lower levels of protein phosphorylation. *Plant Physiol.* **164**, 966–977 (2014).
47. J. Yang, X. Chen, A. McDermaid, Q. Ma, DMINDA 2.0: Integrated and systematic views of regulatory DNA motif identification and analyses. *Bioinformatics* **33**, 2586–2588 (2017).
48. J. Rivoal, A. D. Hanson, Evidence for a large and sustained glycolytic flux to lactate in anoxic roots of some members of the halophytic genus *Limonium*. *Plant Physiol.* **101**, 553–560 (1993).